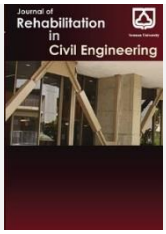

Journal of Rehabilitation in Civil Engineering

Journal homepage: https://civiljournal.semnan.ac.ir/

Comparative Study on Damage Detection for Plate Structures Using Chaotic-TLBO with Multiple Objective Functions

Ali Abedi [1]; Ali Shabani Rad [1]; Gholamreza Ghodrati Amiri [1,2,*]

1. School of Civil Engineering, Iran University of Science and Technology, HengamStreet, Narmak, Tehran, 6765-163, Tehran, Iran
2. Natural Disasters Prevention Research Center, School of Civil Engineering, Iran University of Science and Technology, HengamStreet, Narmak, Tehran, 6765-163, Tehran, Iran
* Corresponding author: *Ghodrati@iust.ac.ir*

ARTICLE INFO

Article history:
Received: 28 September 2024
Revised: 07 April 2025
Accepted: 10 June 2025

Keywords:
Damage detection;
Plate structure;
Chaotic maps;
Modal data;
Chaotic-TLBO.

ABSTRACT

Structural Health Monitoring (SHM) has a crucial role in maintaining the safety and longevity of critical structures, such as buildings, bridges, and aerospace components. Early detection of structural damage, allows for timely intervention, reducing costs and preventing catastrophic failures. This study introduces an innovative approach for damage detection in plate structures by enhancing the Teaching-Learning-Based Optimization (TLBO) algorithm through the integration of chaotic maps. The proposed method, termed Chaotic Teaching-Learning-Based Optimization (CTLBO), leverages the dynamic properties of chaotic maps to improve the algorithm's performance and robustness. The proposed method utilizes modal data to solve an inverse optimization problem, aiming to enhance the accuracy of damage detection. Two benchmark plate structures namely an L-plate with dual clamps and a Rectangular plate with a quarter-circle cutout, are analyzed under noisy and noise-free conditions. Four objective functions, formulated based on modal frequencies and mode shapes, are utilized to quantify the error in damage localization and severity estimation. The effectiveness of the CTLBO algorithm is evaluated against the standard TLBO algorithm. Results demonstrate that CTLBO outperforms TLBO, particularly in noisy environments, achieving near-zero error and offering superior robustness in identifying damage locations and intensities. The findings suggest that the integration of chaotic maps improves the convergence speed and reliability of the TLBO algorithm, making it a promising tool for real-world SHM applications.

E-ISSN: 2345-4423

How to cite this article:
Abedi, A., Shabani Rad, A. and Ghodrati Amiri, G. (2026). Comparative Study on Damage Detection for Plate Structures Using Chaotic-TLBO with Multiple Objective Functions. Journal of Rehabilitation in Civil Engineering, 14(2), 2169 http://doi.org/10.22075/jrce.2025.2169

1. Introduction

Damage detection and SHM have become critical areas of focus across multiple industries, including civil engineering, mechanical engineering, and aerospace. This increased attention stems from the fact that repairing primary structures is generally less expensive than constructing them from the ground up. SHM is a process that typically involves four key steps: (1) determining the presence of damage, (2) identifying its location, (3) quantifying the severity of the damage, and (4) forecasting the remaining useful life of the affected structure Once the presence of damage is diagnosed, accurately localizing the damage becomes paramount in the health monitoring process [1,2].

Damage detection methods are broadly categorized into static-based and dynamic-based approaches, depending on the type of excitation and the data used in the detection process. The practical challenges in implementing and acquiring data for static-based methods have led researchers to explore more feasible inspection and prognosis techniques using structural dynamics or vibration characteristics. Modal data-based approaches represent a subset of vibration-based methods, where the detection theory is grounded in the relationship between a structure's physical properties and its modal characteristics. Any alterations in the physical properties of the system result in observable changes in the modal data, such as frequencies and mode shape vectors, which can be employed for detecting structural damage at the component level [3–6]. Modal data-based damage detection methods can be divided into two primary categories: deterministic methods and iterative approaches. The simplest deterministic method involves examining changes in resonant frequencies to identify and/or quantify significant damage. Additionally, combinations of mode shapes and vibration frequencies have been employed as one-step, deterministic techniques for damage detection [7–11]. The success of these methods highly depends on the sensitivity of the modes to the occurred damage. Consequently, deterministic methods frequently encounter limitations in accurately quantifying damage. They often yield only approximate estimates unless high-frequency content is incorporated as structural feedback during the excitation process. In contrast, iterative methods, which treat damage detection as an inverse problem of model updating, can overcome the limitations of deterministic approaches. One of the most effective techniques is Finite Element Method (FEM), where damage-related parameters are treated as unknown variables at the element level, and the numerical model is updated to match the behaviour of the monitored structure. Optimization algorithms are instrumental in solving this model updating problem, formulated as an error minimization process between the real structure and its analytical model [12–15].

Over the past few decades, various methods which utilize modal data have been introduced to identify and localize structural damage. Modal analysis, which examines the inherent vibrational properties of a structure, has proven to be a powerful tool in this regard [16]. By analysing shifts in modal parameters, engineers can gain valuable insights into the integrity of a structure and detect areas of concern before they lead to catastrophic failure [17–19]. As the field of SHM continues to evolve, the integration of advanced technologies, such as machine learning and sensor networks, is expected to enhance further the accuracy and efficiency of damage detection and health monitoring processes [20–22].

In recent decades, many researchers have used inverse optimization problems with metaheuristics algorithms to detect the presence of damage, specify the damage intensity, and localize the damage [23,24]. For instance, Vaez et al. [25] introduce a hybrid genetic–particle swarm optimization algorithm for detecting damage, its location, and severity in plate structures. Three numerical examples, including different types of plates, are simulated using thin plate theory, with objective functions formulated based on modal data. Their results show that the hybrid algorithm performs better than genetic and Particle Swarm Optimization (PSO) algorithms individually, as indicated by lower error rates. Mohamadinasab et al. [26] examine the impact of structural asymmetry on damage detection by modelling symmetric and asymmetric truss and

frame structures with various damage scenarios. It compares the effectiveness of three objective functions (based on flexibility matrix, natural frequency, and modal frequency) optimized using the multiverse optimizer. The findings reveal that asymmetry improves damage detection accuracy in some instances, particularly for truss and frame models with differing span lengths. Fan et al. [27] present an algorithm based on 2D continuous wavelet transform for detecting damage in plate-type structures. It uses isosurfaces of wavelet coefficients to identify the location and shape of damage from the mode shapes of plates. The method shows superior noise immunity and robustness compared to other techniques and is validated in both numerical and experimental tests.

Xiang et al. [28] propose a two-step approach for detecting multiple damage in thin plates. First, 2-D wavelet transform is applied to modal shapes to locate damage, followed by PSO to assess damage severity. Their study, based on wavelet FEM simulations, evaluates the method's effectiveness even with imprecise natural frequency measurements, suggesting that higher and more natural frequencies improve damage severity evaluation. Seyedpoor et al. [29] propose a method for accurately locating structural damage by integrating optimal sensor placement and a Modal Strain Energy-Based Index (MSEBI). They use the binary differential evolution algorithm to optimize sensor placement and apply MSEBI to identify damage based on the optimal setup.

While optimization-based model updating methods offer strong performance, they also come with several limitations. Key issues include the tendency to become trapped in local extrema, high sensitivity to noisy data, and slow convergence, which can significantly hinder their effectiveness. Addressing these challenges is critical for advancing damage detection techniques, especially in applications requiring high accuracy and reliability under real-world conditions. To bridge these gaps, this study introduces chaotic maps into TLBO to solve the inverse optimization problem of damage detection in plate structures. The use of chaotic maps is a novel approach aimed at overcoming the inherent limitations of traditional TLBO, such as poor exploration capabilities and reduced performance in noisy scenarios. Chaotic maps generate complex, non-repetitive sequences that improve exploration, helping avoid local optima and maintaining search diversity. This balance between exploration and exploitation enhances the algorithm’s search efficiency and robustness.

The significance of this research lies in its potential to enhance the effectiveness of optimization algorithms for SHM by integrating chaotic maps into TLBO, we aim to provide a more robust solution for accurately detecting damage in plate structures, even in the presence of noise. The study evaluates this approach using two thin plate benchmarks (an L-plate with dual clamps and a Rectangular plate with a quarter-circle cutout) to assess its impact on accuracy, convergence speed, and noise resilience. These contributions not only address key shortcomings in optimization-based damage detection methods but also offer a practical framework for improving structural integrity assessments in engineering applications.

The rest of the paper is organized as follows: section 2 explains the damage detection approaches and dynamic background of the problem. Section 3 presents a brief explanation of the CTLBO, and section 4 introduces two numerical examples to validate the effectiveness of the proposed algorithm and compare the results in noisy and noise-free states.

2. Theoretical backgrounds

The damage detection process involves addressing the inverse optimization problem by leveraging the structure's dynamic parameters. This section focuses on formulating the problem and outlining the methodology, with an emphasis on determining practical objective functions to quantify and localize damage.

2.1. Methodology for damage identification

FEM is a widely used technique for solving direct structural problems, where the input, such as an applied load, is used to determine the resulting structural responses, such as strains. Moreover, when a structure sustains damage, its structural properties change, deviating from those of its original, undamaged state. Therefore, damage detection relies on an inverse method, which aims to solve optimization problems by analyzing structural properties. This approach uses an objective function that is integrated into an optimization algorithm. By minimizing this function, the algorithm can identify and estimate the parameters related to the damage. Ultimately, the suggested damage detection strategy involves addressing an optimization problem that incorporates the structure's dynamic properties and the objective function, as outlined in a sequence of steps illustrated in Fig. 1.

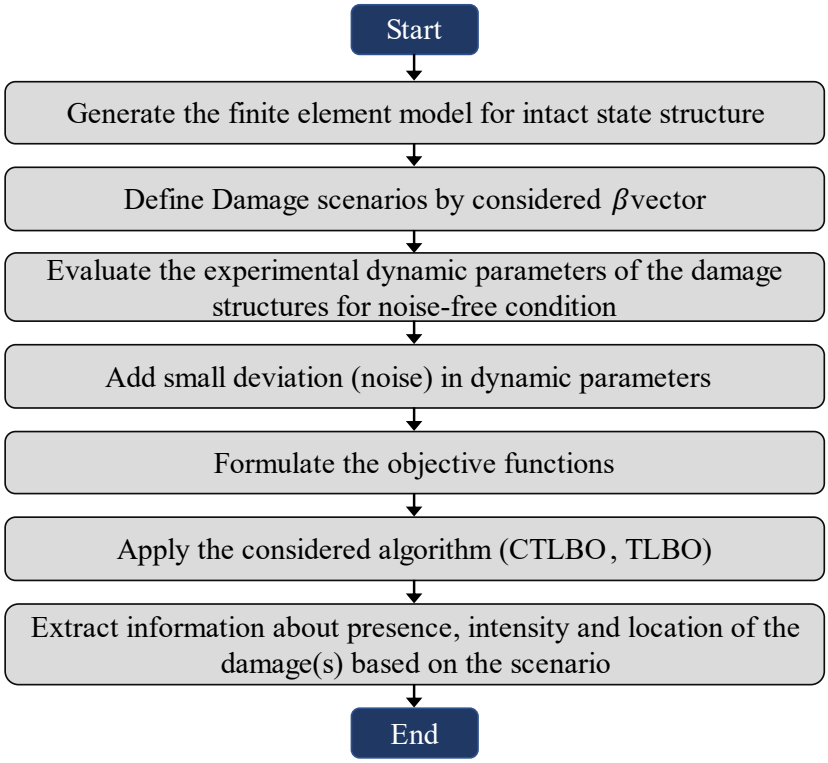

Fig. 1. Damage detection approach.

To develop a finite element model, it is necessary to compute the global stiffness matrix, K, and mass matrix, M, for the structure through Eqs. 1 and 2 [30]:

$$K = \sum_{i=1}^{NE} K_i \quad (1)$$

$$M = \sum_{i=1}^{NE} M_i \quad (2)$$

where NE represents the total count of elements. This research models plate structures by applying thin plate theory. The representation of the plates is achieved through Constant Strain Triangle (CST) elements under plane stress assumptions. Consequently, a typical element's stiffness and mass matrices, as depicted in Fig. 2, are formulated based on Eqs. 3 and 4 [31,32].

$$k^e = t_e A_e B^T D B \tag{3}$$

$$m^e = \frac{\rho_e A_e}{12}\begin{bmatrix} 2 & 0 & 1 & 0 & 1 & 0 \\ 0 & 2 & 0 & 1 & 0 & 1 \\ 1 & 0 & 2 & 0 & 1 & 0 \\ 1 & 0 & 1 & 0 & 2 & 0 \\ 1 & 0 & 1 & 0 & 2 & 0 \\ 0 & 1 & 0 & 1 & 0 & 2 \end{bmatrix} \tag{4}$$

where t_e, ρ_e, and A_e are the element's thickness, mass density, and area, accordingly. B is known as the strain-displacement matrix which relates the nodal displacements to the strains within an element. Also, D is the constitutive matrix (or stress-strain matrix) used to relate stresses to strains. B is a 3×6 matrix, and D is a 3×3 matrix, specifically for planar stress conditions, which are formulated according to Eqs. 5 and 6 [32,33]:

$$B = \frac{1}{det\, J}\begin{bmatrix} y_{23} & 0 & y_{31} & 0 & y_{12} & 0 \\ 0 & x_{32} & 0 & x_{13} & 0 & x_{21} \\ x_{32} & y_{23} & x_{13} & y_{31} & x_{21} & y_{12} \end{bmatrix} \tag{5}$$

$$D = \frac{E}{1-\nu^2}\begin{bmatrix} 1 & \nu & 0 \\ \nu & 1 & 0 \\ 0 & 0 & \frac{1-\nu}{2} \end{bmatrix} \tag{6}$$

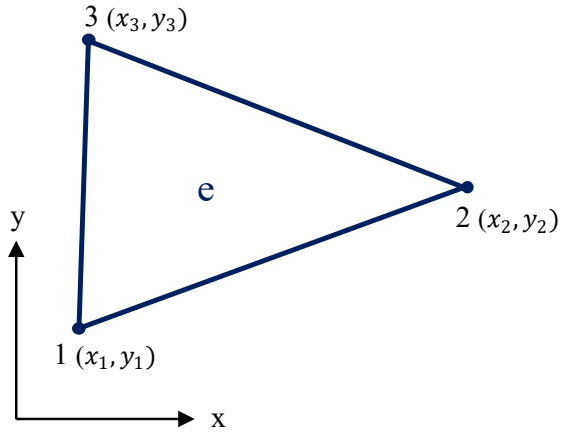

Fig. 2. typical triangle element.

where x_{ij} and y_{ij} are the differences between the x and y coordinates of nodes i and j, respectively. Poisson's ratio is represented by ν, and E is the modulus of elasticity. J is the Jacobian matrix of the transformation, which can be expressed as Eq. 7 [34]:

$$J = \begin{bmatrix} x_{13} & y_{13} \\ x_{23} & y_{23} \end{bmatrix} \tag{7}$$

In this study, damage is considered as a stiffness reduction which directly affects the elasticity module. Therefore, to implement the damage scenario, the damage vector, β, with dimension of $1 \times n$ is constructed, where n is the element number. This numerical value in the ith position of this vector indicates the extent of damage to the ith structural component. This value ranges from 0 to 1, with 0 indicating a completely intact element and 1 indicating a wholly damaged element. Therefore, the relationship between the intact (subscript h) and damaged state (subscript d) of the structure can be formulated as Eq. 8 [12]:

$$E_{id} = (1 - \beta_i \times 1) \times E_{ih} \tag{8}$$

Finally, the dynamic parameters can be expressed by modifying the ith eigenvalue equation for the damaged structure, as shown in Eq. 9 [30,35]:

$$\left(K_d - \omega_{id}^2 M\right)\Phi_{id} = \{0\}_{n\times 1} \tag{9}$$

where ω_{id} represent the ith natural frequency and ϕ_{id} is its corresponding mode shape for damaged condition. To consider uncertainties and push the study to real word conditions, small white noise is produced and added to both the frequencies and mode shapes of the structures. This process is implemented using Eqs. 10 and 11 [3]:

$$\omega_{noisy} = \omega_{id}\left(1 + \alpha \times \text{noise}_{freq}\right) \tag{10}$$

$$\Phi_{ij,noisy} = \Phi_{i,j,d}(1 + \alpha \times noise_{mode}) \tag{11}$$

here, α is a uniformly distributed random number between -1 and +1. In this study, 1% noise is selected to investigate its effect on the results.

2.2. Objective Functions

In this section, four well-known objective functions are selected and compared to each other to minimize the error in solving the inverse optimization problem of damage detection. The first objective function taken from Mohamadinasab et al. [26] is formulated as Eq. 12:

$$F_1 = \sum_{i=1}^{nm}\left(\frac{\omega_i^d - \omega_i^u}{\omega_i^u} - \frac{\omega_i^m - \omega_i^u}{\omega_i^u}\right)^2 \tag{12}$$

Where superscripts u and m in Eq. 12 refer to the undamaged and analytical model of the structure. nm denotes the number of considered mode shapes for damage detection.

The second function can be defined according to Eq. 13, calculated using the flexibility matrix obtained by Eq. 14.

$$F_2 = \frac{1}{nd}\sum_{i=1}^{nd}\left\|FM_i^d - FM_i^m\right\| \tag{13}$$

$$FM = \phi_{nm}\Lambda_{nm}^{-1}\phi_{nm}^T \tag{14}$$

Where Λ_{nm} is the diagonal matrix of eigenvalues of the first nm modes, and superscript T denotes the transpose of the matrix.

The third objective function can be written by using frequencies as Eq. 15:

$$F_3 = \sqrt{\frac{\sum_{i=1}^{nm}\left(f_i^d - f_i^m\right)^2}{nm}} \tag{15}$$

In Eq. 15, f_i indicates the frequencies which can be defined as corresponding natural frequencies according to Eq. 16.

$$f_i = \frac{\omega_i}{2\pi} \tag{16}$$

Following the approach of Vaez and Fallah [25], the fourth objective function can be defined as Eq. 17, which utilizes natural frequencies and mode shapes in each degree of freedom in a set of selected modes.

$$F_4 = \sqrt{\frac{1}{nm}\left(\sum_{i=1}^{nm}\left(\omega_i^{ex} - \omega_i^{gp}\right)^2 + \sum_{i=1}^{n}\sum_{j=1}^{nd}\left(\phi_{ij}^{ex} - \phi_{ij}^{gp}\right)^2\right)} \tag{17}$$

The objective function F_4 serves as a quantitative measure to assess the discrepancy between experimental observations and the results obtained through the CTLBO algorithm. Specifically, values with the superscript *ex* refer to experimentally determined results, which are considered as the reference or ground truth data. In contrast, the superscript *gp* corresponds to the outcomes predicted or computed using the

optimization process guided by the CTLBO algorithm. The variable *n* represents the total number of natural vibration modes considered in the analysis, whereas *nd* indicates the degrees of freedom included in the objective function. These two parameters control the computational cost with respect to the accuracy of the optimization process. Similarly, ϕ_{ij} , representing the *j*th mode shape of the *i*th degree of freedom, provides a spatial representation of how the structure deforms during vibration. Comparing ϕ_{ij}^{ex} and ϕ_{ij}^{gp} allows for a detailed assessment of the algorithm's ability to replicate the structural behavior.

2.3. Chaotic systems and maps

For much of history, scientists viewed the world as a collection of systems that operated predictably under the laws of nature. However, advancements in science revealed that many natural phenomena could not be explained by these deterministic views. This led to the development of chaos theory in mathematics, which focuses on systems whose behaviour is highly sensitive to initial conditions, making their future outcomes unpredictable. These non-linear dynamic systems, often referred to as chaotic systems, include examples like the butterfly effect, air currents, and economic cycles. The core principle of chaos theory is that disorder often contains an underlying order, even if it is not immediately apparent. On a larger scale, systems that appear random at a local level may exhibit stable and predictable behavior. This concept shares similarities with statistics, which also seeks patterns within apparent randomness. For example, while each coin toss produces a random result, the aggregate outcome over many tosses becomes predictable. Similarly, scientific predictions, such as those for earthquakes, may seem random in the short term but reveal periodic patterns over extended timeframes, such as 500 or 2400 years [36–38].

In many meta-heuristic algorithms, results tend to improve gradually and often get stuck at local optima, leading to premature convergence. In other words, the two critical phases of exploration and exploitation are crucial for converging on optimal solutions. An imbalance between these phases can reduce the algorithm's effectiveness. Chaotic sequences provide a way to escape this issue by introducing disorder into the search space, allowing the algorithm to explore more diverse and widespread regions. As a result, the local optima are less likely to capture the search process. Chaotic sequences are generated from specific chaotic functions, and although they do not exhibit random behaviour, they introduce complex, irregular patterns in the search space. These sequences are mainly characterized by sensitivity to initial conditions, as well as non-periodic and ergodic behaviours, with no inverse functions. Several well-known chaotic maps, such as Logistic, Tent, Gaussian, Liebovitch, Chebyshev, Sinusoidal, and Piecewise, can be embedded into meta-heuristic algorithms. Among these, in this study, the Chebyshev function was determined to be the most effective through trial and error [39].

3. CTLBO algorithm

TLBO is an optimization algorithm inspired by the teaching and learning process in a classroom. It was developed by R.V. Rao, V.J. Savsani, and D.P. Vakharia [40] in 2011. The algorithm simulates the influence of a teacher on the learners (students) in a class. The process is divided into the "Teacher Phase" and the "Learner Phase". In the Teacher Phase, the algorithm identifies the best solution (teacher) and tries to improve the mean performance of the entire class by adjusting the learners' solutions based on the difference between the teacher's knowledge and the average knowledge of the class. In the Learner Phase, learners update their solutions by interacting with each other, emulating how students learn from their peers. In the Teacher Phase, the algorithm updates each learner's solution X_{new} based on the teacher's solution X_{best} using the following formula [40]:

$$X_{new} = X_{old} + r \cdot \left(X_{best} - T_f \cdot M\right) \quad (18)$$

where X_{old} is the current solution, r is a random number in the range [0,1], T_f is the teaching factor (either 1 or 2, chosen randomly), and M is the mean of the current solutions in the class. This formula ensures that the influence of the teacher pulls the learners' solutions towards a better solution, thereby improving the overall quality of solutions. Fig. 3 illustrates the TLBO algorithm, which forms the basis of CTLBO. In CTLBO, all instances of random number generation in learner phase are replaced with chaotic sequences (e.g., using a Chebyshev map) to improve exploration and prevent premature convergence.

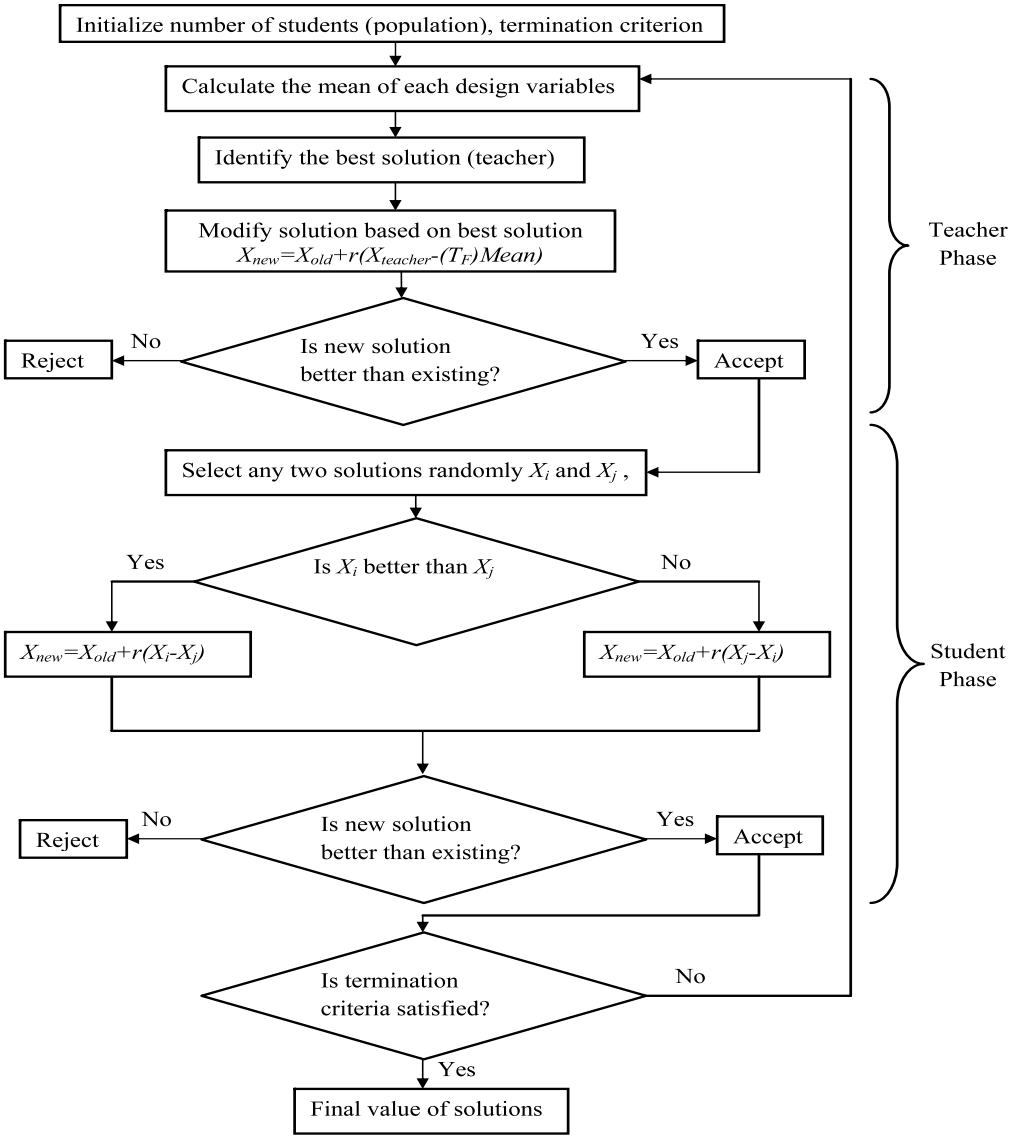

Fig. 3. Flowchart for TLBO [40].

The strength of the TLBO algorithm lies in its simplicity and efficiency. It does not require algorithm-specific parameters like crossover probability in Genetic Algorithms or inertia weight in PSO algorithm. This parameter-free nature makes TLBO easier to implement and tune across different problem domains. Additionally, because of its balance between exploration and exploitation, TLBO has been shown to perform well across various optimization problems, including those with complex, multi-modal landscapes. The algorithm's ability to guide the search process effectively through both teacher and peer learning phases contributes to its robustness and effectiveness in finding global optima. Note that in this algorithm, a chaotic map (Chebyshev) is used everywhere the algorithm produces random numbers.

To provide more detail on how the algorithm operates during code execution, each algorithm run is structured to minimize the objective functions iteratively. Specifically, the process starts by generating a set of initial candidate solutions that represent potential damage scenarios within the plate structure. These solutions are evaluated against the defined objective functions to determine their performance. The algorithm updates these solutions during each iteration based on its learning phases. For TLBO, this involves the teacher phase, where the best current solution influences the others to improve towards a higher mean, and the learner phase, where solutions are further refined through pairwise interactions. In CTLBO, chaotic maps are integrated to introduce complex, non-repetitive sequences during the update process.

The iterative process of calculating, updating, and comparing solutions continues until the specified Number of Function Evaluations (NFEs) is completed. This systematic approach allows the algorithms to converge towards an optimal or near-optimal solution for identifying damage in the structure. Table 1 provides a pseudo-code implementation of the algorithm.

Table 1. Pseudo-code.

Algorithm 1 CTLBO	
Learning phase	
1	**For** $i = 1{:}\, P_n$
2	Randomly select two learners X_i and X_j, where ($i \neq j$) Use chaotic sequences to influence how they learn from each other
3	If $f(X_i) < f(X_j)$
4	$X_{\text{new},i} = X_{\text{old},i} + r_i(X_i - X_j)$
5	Else
6	$X_{\text{new},i} = X_{\text{old},i} + r_i(X_j - X_i)$
7	End if
8	End for Accept X_{new} if it gives a better function value.

4. Numerical example and validation

In this section, an L-plate with dual clamps and Rectangular plate with a quarter-circle cutout, as illustrated in Fig. 4 and Fig. 5, respectively, are simulated using MATLAB 2022a to evaluate the effectiveness of the proposed CTLBO algorithm. The performance is compared with the standard TLBO algorithm in both noisy and noise-free conditions.

4.1. An L-plate with dual clamps

The first plate consists of 32 CST elements. In this plate, five frequencies and their corresponding mode shapes are considered in the analysis. This choice strikes a balance between computational efficiency and the algorithm's accuracy. Additionally, the material attributes of the plate are detailed in Table 2. The termination criterion is set based on a fixed NFEs to ensure consistency and fairness between the scenarios.

The following damage scenarios are assumed for the plate:

Scenario 1: Element 16 experiences a 20% damage.

Scenario 2: Element 9 undergoes a 10% damage, while element 32 experiences a 12% reduction.

Table 2. Material attributes of the thin plates.

Property (*unit*)	value
E, elasticity modules (GPa)	210
ρ, mass density (kg/m^3)	7850
ν, Poisson's ratio	0.3

t, thickness (*m*)	0.005

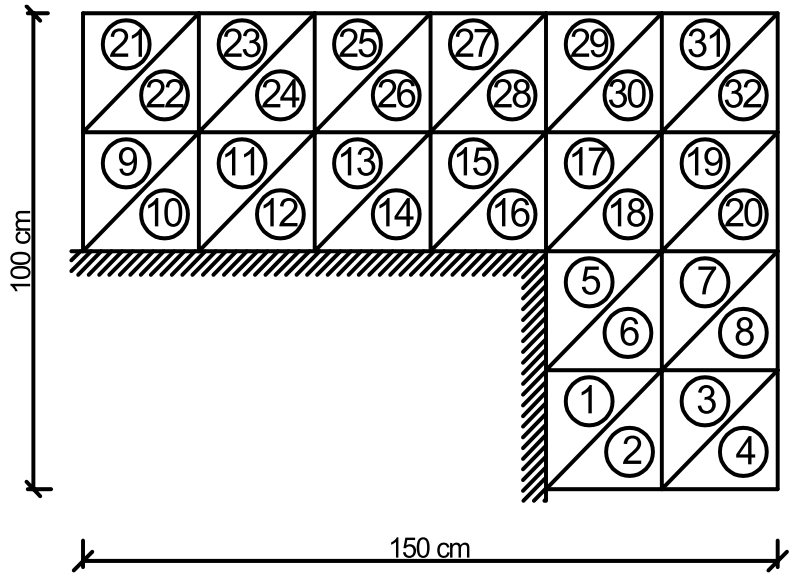

Fig. 4: An L-plate with dual clamps [25].

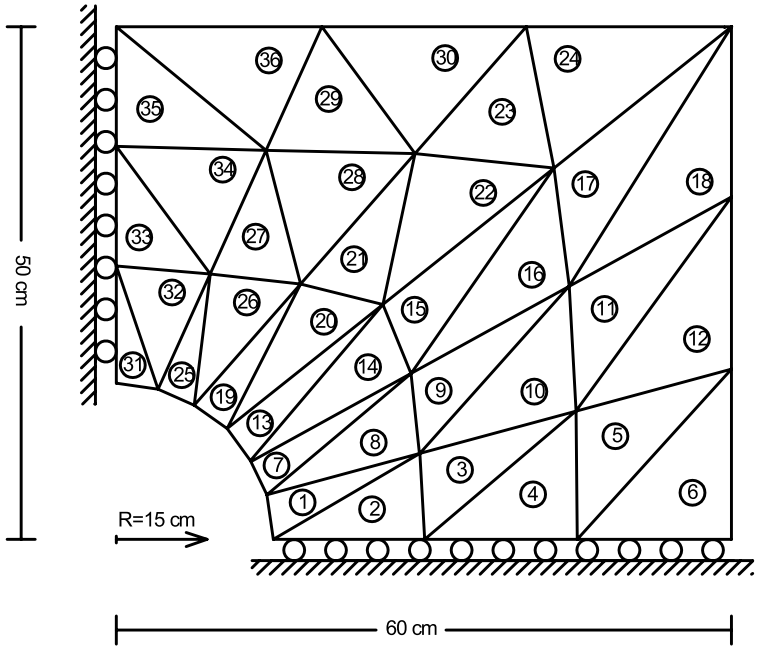

Fig. 5: Rectangular plate with a quarter-circle cutout [25].

4.2. Rectangular plate with a quarter-circle cutout

The second plate consists of 36 CST elements. In this plate, similar to the first plate, the analysis incorporates five frequencies and their corresponding mode shapes, chosen to balance computational efficiency and algorithm accuracy. The material attributes of this plate are also provided in Table 2. The following damage scenarios are considered for the plate:

Scenario 1: Element 7 is subjected to a 6% damage.

Scenario 2: Element 13 experiences a 15% damage, while element 24 undergoes a 10% damage.

4.3. Results and discussion

The damage detection procedure was performed across 20 individual runs, with the best results for each algorithm and each scenario for both plates.

For the first plate, the damage detection outcomes are illustrated in Figs. 6 and 7 for scenarios 1 and 2, respectively, with the corresponding loss value results summarized in Table 3.While both TLBO and CTLBO successfully identify the damaged elements, it is evident that TLBO faces significant challenges, particularly in noisy conditions, where its accuracy and reliability diminish noticeably compared to CTLBO. In Scenario 1, under noise-free conditions, CTLBO attains the minimum loss values across all objectives, significantly outperforming TLBO, which exhibits non-negligible losses particularly in F_1 and F_3. CTLBO also shows significantly lower losses in noisy conditions than TLBO, indicating better noise handling across all objectives. In Scenario 2, CTLBO consistently outperforms TLBO in both noisy and noise-free conditions. TLBO exhibits high losses, particularly in noisy conditions, while CTLBO reduces these losses substantially, especially in F_1 and F_3.

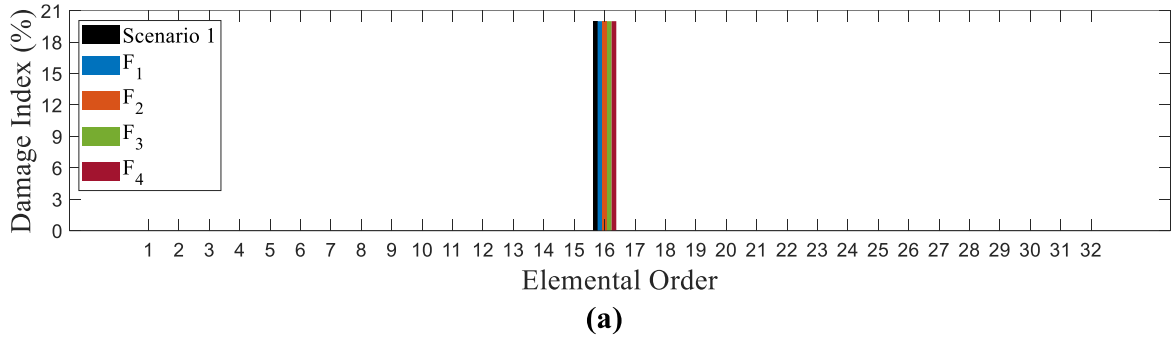

(a)

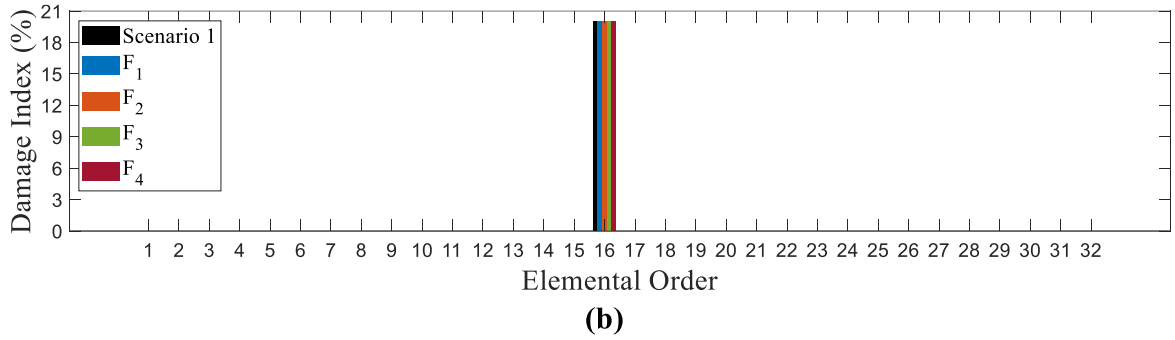

(b)

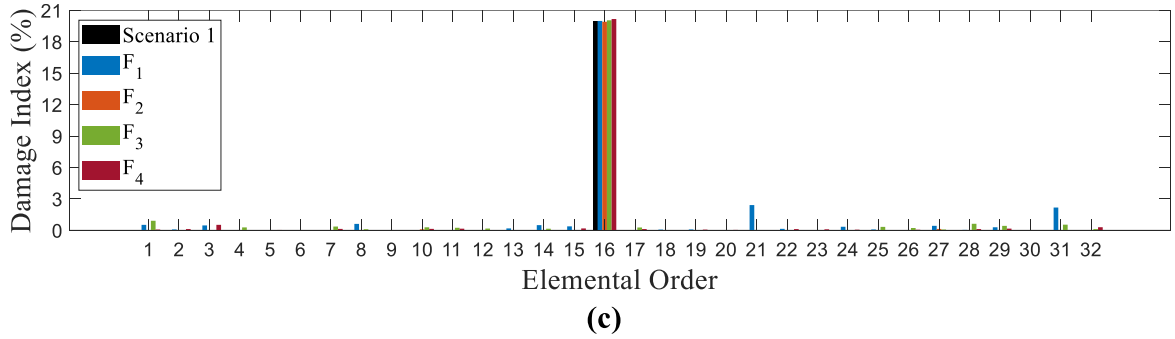

(c)

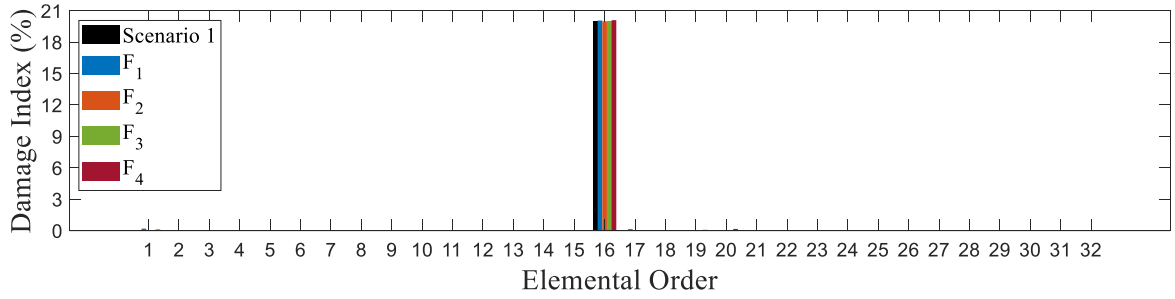

(d)

Fig. 6. Damage detection and localization results of the L-plate with dual clamps for scenario 1: (a) TLBO, (b) CTLBO, (c) TLBO with noise, (d) CTLBO with noise.

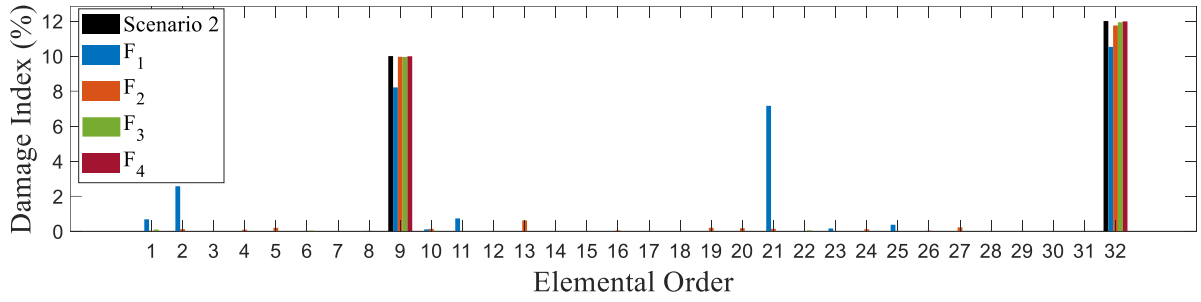

(a)

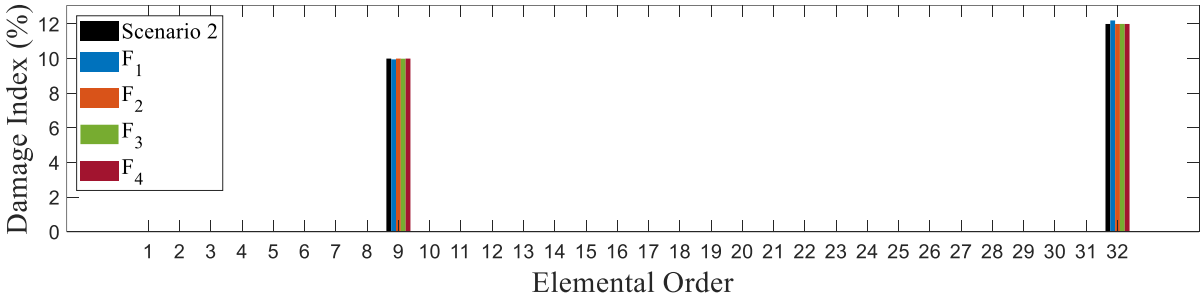

(b)

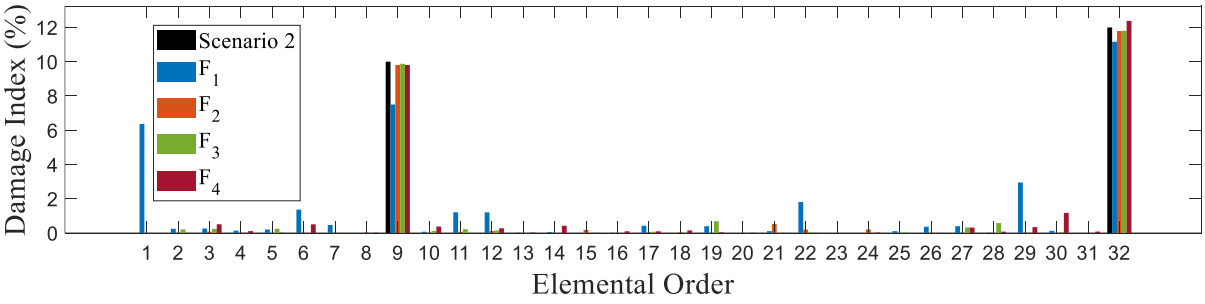

(c)

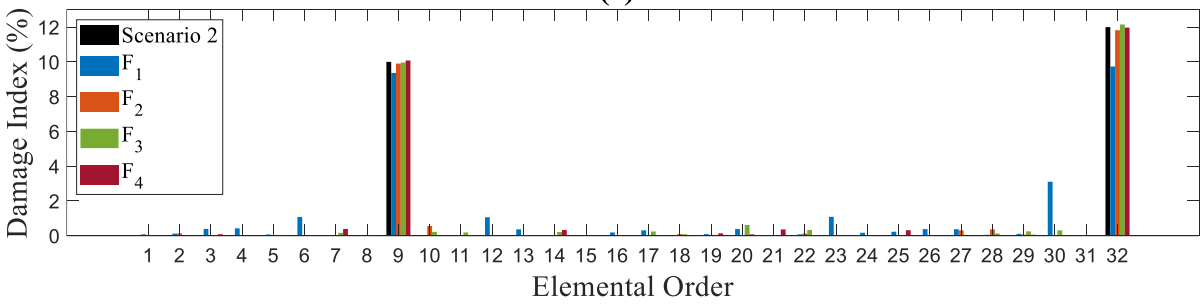

(d)

Fig. 7. damage detection and localization results of the L-plate with dual clamps for scenario 2: (a) TLBO, (b) CTLBO, (c) TLBO with noise, (d) CTLBO with noise.

Table 3. Loss value results of the L-plate with dual clamps.

	Scenario 1			
	F1	F2	F3	F4
TLBO	0.0003±0.0000	0.0000±0.0000	0.0020±0.0000	0.0000±0.0000
CTLBO	0.0000±0.0000	0.0000±0.0000	0.0000±0.0000	0.0000±0.0000
TLBO-N	0.2718±0.0034	0.4194±0.0026	0.2632±0.0537	0.8725±0.0271
CTLBO-N	0.0455±0.0905	0.1025±0.0010	0.1424±0.0000	0.4453±0.0051
	Scenario 2			
	F1	F2	F3	F4
TLBO	30.1574±0.1186	2.53242±0.0227	1.0679±0.0025	0.2694±0.0005
CTLBO	2.1477±0.0006	0.0000±0.0000	0.0901±0.0003	0.0008±0.0000
TLBO-N	31.9891±0.1840	3.6752±0.0162	1.6378±0.0293	5.1068±0.0482
CTLBO-N	25.2805±0.1026	2.4805±0.0188	2.8242±0.0320	1.0460±0.0194

Note: N corresponds to the noisy condition.

Table 4. Loss value results of the Rectangular plate with a quarter-circle cutout.

	Scenario 1			
	F_1	F_2	F_3	F_4
TLBO	0.0135+0.0000	0.0000+0.0000	7.0835+0.0105	0.0123+0.0000
CTLBO	0.0003+0.0000	0.0000+0.0000	0.0000+0.0000	0.0000+0.0000
TLBO-N	3.9280+0.0132	0.0007+0.0033	1.4780+0.0111	6.5692+0.0235
CTLBO-N	0.0181+0.0000	0.0027+0.0000	0.0157+0.0001	0.6611+0.0013
	Scenario 2			
	F_1	F_2	F_3	F_4
TLBO	0.0802 +0.0004	0. 6434+0.0037	0.0010+0.0000	0.1259+0.0001
CTLBO	0.0009 +0.0000	0.0194+0.0002	0.0000+0.0000	0.0000+0.0000
TLBO-N	8.5614+0.0140	13.136+0. 1410	1.3132+0.0045	0.4574+0.0016
CTLBO-N	0.4998+0.0006	2.7010+0.0059	0.9726+0.0006	0.2425+0.0008

Note: N corresponds to the noisy condition.

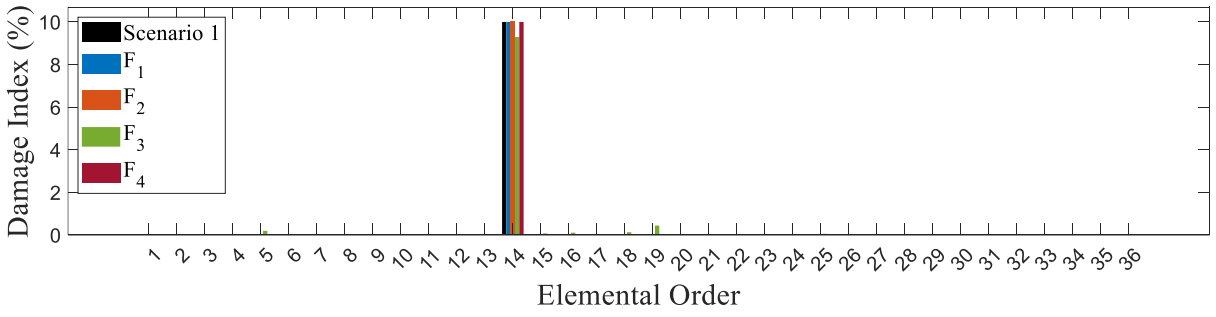

(a)

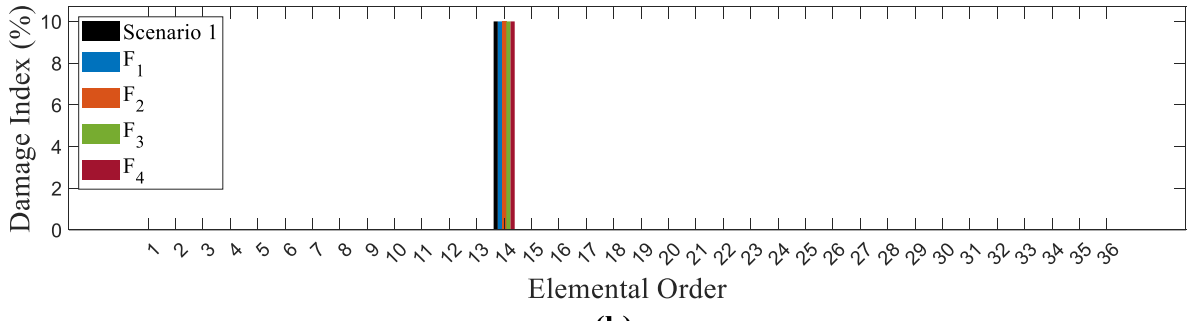

(b)

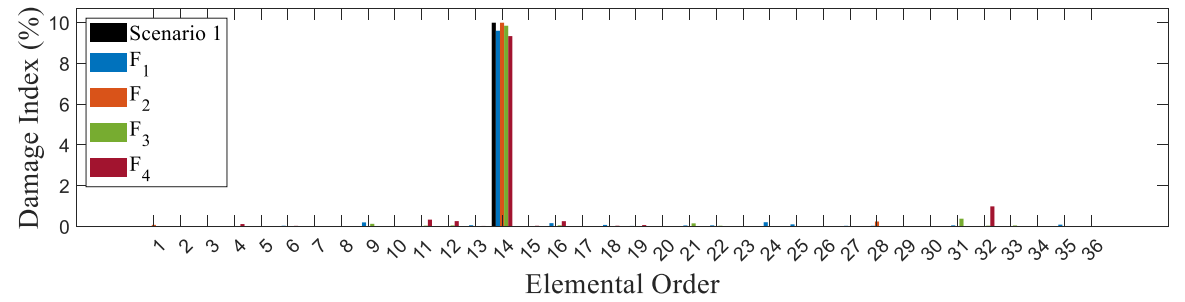

(c)

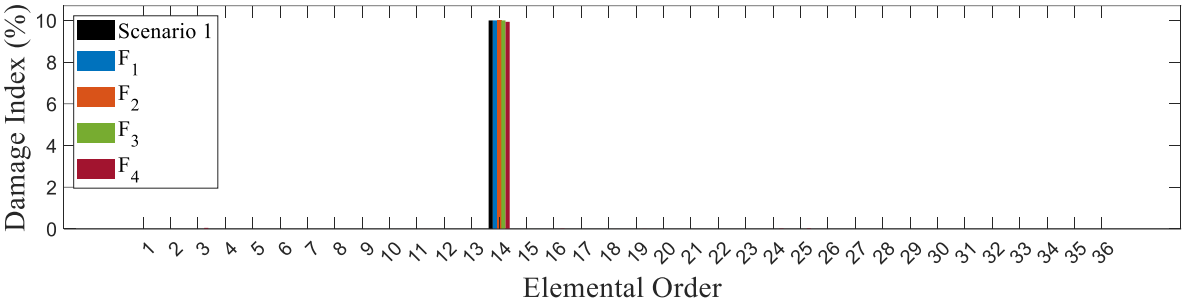

(d)

Fig. 8. Damage detection and localization results of the Rectangular plate with a quarter-circle cutout for scenario 1: (a) TLBO, (b) CTLBO, (c) TLBO with noise, (d) CTLBO with noise.

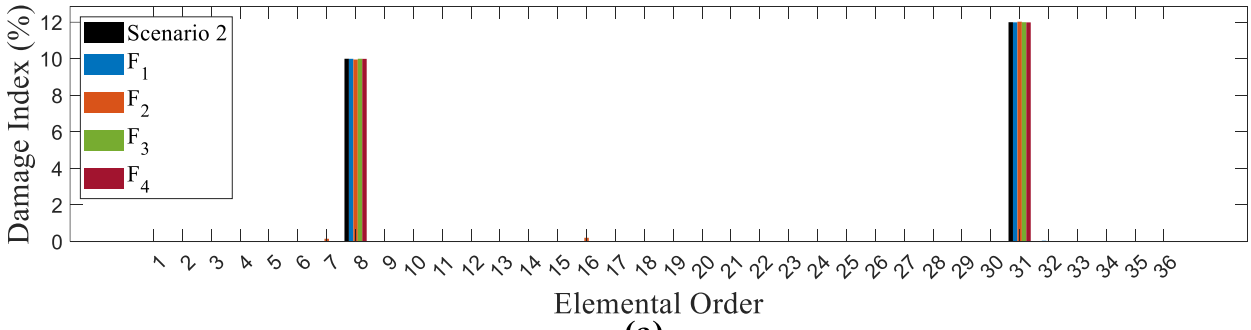

(a)

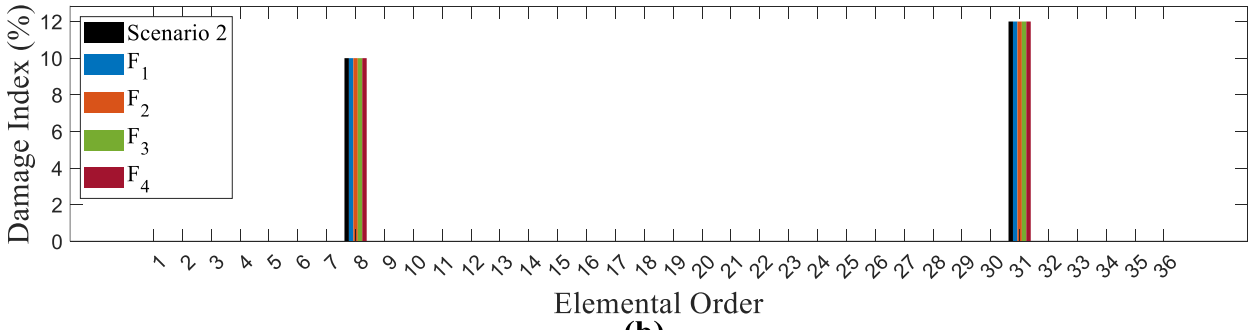

(b)

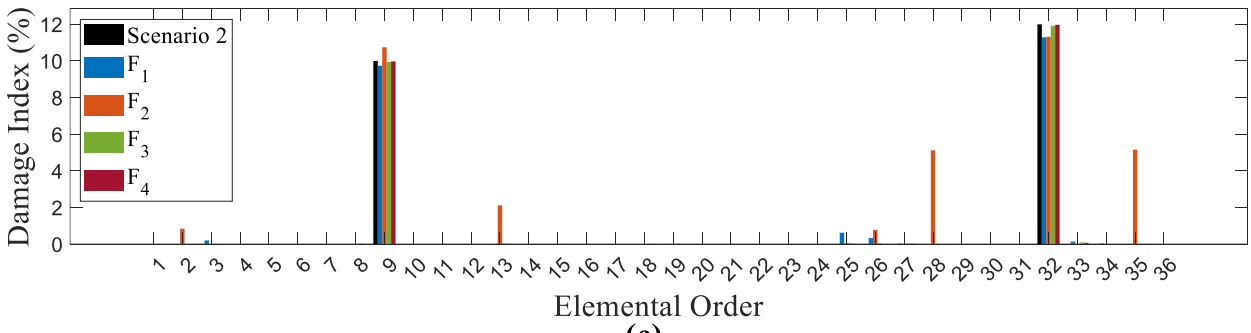

(c)

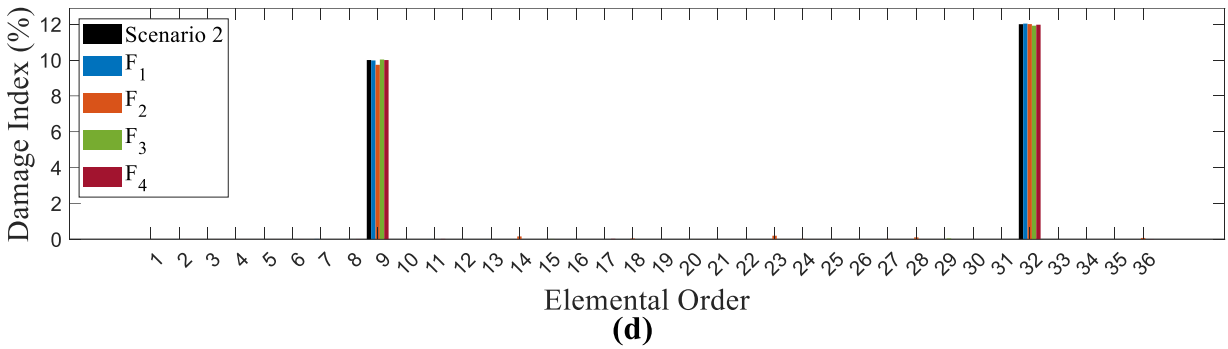

Fig. 9. Damage detection and localization of the Rectangular plate with a quarter-circle cutout for scenario 2: (a) TLBO, (b) CTLBO, (c) TLBO with noise, (d) CTLBO with noise.

For the second plate, objective functions' error values are listed in Table 4, and damage detection results for both scenario 1 and scenario 2 are presented in Figs. 8 and. 9, respectively. The findings demonstrate that while both algorithms identified the damage elements with acceptable accuracy, CTLBO consistently outperforms TLBO in both noisy and noise-free conditions across all objective functions F_1, F_2, F_3, and F_4 in both scenarios. In Scenario 1, CTLBO achieves near-zero losses across all objectives, while TLBO shows moderate losses, particularly in F_3. Under noisy conditions, CTLBO reduces losses significantly compared to TLBO, especially in F_1 and F_4. A similar trend is observed in Scenario 2, where CTLBO exhibits superior performance by minimizing losses across all objectives in noisy and noise-free states.

Fig. 10 illustrates the convergence curves for the second objective function under noisy conditions in Scenario 2 for two benchmark plates. These figures highlight the comparative performance of TLBO and CTLBO in tackling noise-affected structural damage detection problems.

In Fig. 10 (a), which corresponds to the L-plate with dual clamps, CTLBO demonstrates a significantly faster and more stable convergence compared to TLBO. CTLBO rapidly achieves lower objective function values within the early stages of optimization (around 50 NFEs), stabilizing at a value several magnitudes smaller than that of TLBO. In contrast, TLBO exhibits a slower convergence trajectory and plateaus at a higher objective function value, highlighting its reduced capability to navigate noisy conditions effectively. Fig. 10 (b), representing the Rectangular plate with a quarter-circle cutout, presents a similar pattern. CTLBO outperforms TLBO in terms of both speed and accuracy, achieving a remarkably lower objective function value. Notably, CTLBO achieves convergence within fewer NFEs and maintains a steady decline without significant oscillations, even under noisy conditions. Meanwhile, TLBO struggles with erratic progress, leading to a higher final objective function value.

These results confirm the superior performance of CTLBO especially in noisy environments, demonstrating its enhanced convergence speed and precision. The effectiveness of CTLBO is attributed to the incorporation of chaotic maps, which bolster its exploration and exploitation capabilities, enabling it to identify optimal solutions more reliably.

In noisy environments, CTLBO demonstrates improved performance primarily because the integration of chaotic maps enhances exploration by generating a diverse set of candidate solutions. This increased diversity helps prevent premature convergence to local minima that noise can exacerbate in traditional TLBO. However, our analysis also suggests that the advantages of CTLBO might diminish under extremely high noise levels or if the chaotic map parameters (e.g., initial conditions) are not optimally tuned, as these factors could lead to instability in the chaotic sequences.

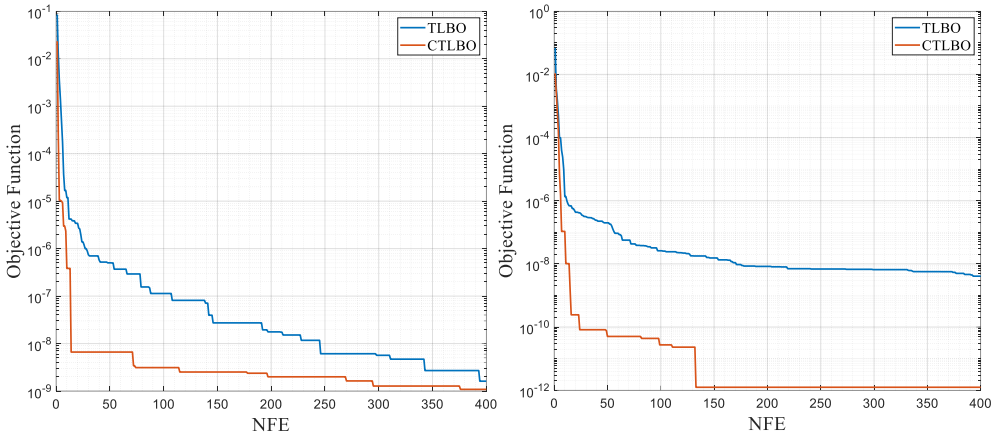

Fig. 10. As representative sample convergence curve of the second objective function for (a) the L-plate with dual clamps under noisy conditions in Scenario 2, and (b) the Rectangular plate with a quarter-circle cutout under noisy conditions in Scenario 2.

5. Conclusion

This study has explored the effectiveness of the CTLBO algorithm for damage detection in plate structures. By introducing chaotic maps into the TLBO framework, we aimed to overcome the common challenges faced by optimization algorithms, such as slow convergence and susceptibility to noise. The numerical experiments on an L-plate with dual clamps and a Rectangular plate with a quarter-circle cutout demonstrate that CTLBO significantly improves the accuracy and robustness of damage detection, particularly in noisy conditions. Four objective functions were considered for evaluating performance. Compared to the traditional TLBO, CTLBO shows superior performance in both noise-free and noisy environments, consistently achieving more accurate damage localization and intensity estimation. The chaotic maps enhance the algorithm's ability to escape local optima, improving overall search efficiency. These findings indicate that CTLBO is a reliable and effective tool for complex SHM applications. It is important to note that the structural models employed rely on simplified assumptions, including moderate noise levels, idealized edge conditions, and plane stress formulations. Future work should explore these complexities to further validate and enhance the method’s applicability to real-world structures.

Funding

This research did not receive any specific grant from funding agencies in the public, commercial, or not-for-profit sectors.

Conflicts of interest

The authors declare that they have no known competing financial interests or personal relationships that could have appeared to influence the work reported in this paper.

Authors contribution statement

Ali Abedi: Methodology, Software, Validation, Writing – original draft, Writing - review & editing, Visualization, Investigation.

Ali Shabani Rad: Methodology, Software, Visualization, Investigation.

Gholamreza Ghodrati Amiri: Conceptualization, Investigation, Project administration, Visualization**,** Supervision.

References

[1] Abdeljaber O, Avci O, Kiranyaz S, Gabbouj M, Inman DJ. Real-time vibration-based structural damage detection using one-dimensional convolutional neural networks. J Sound Vib 2017;388:154–70.

[2] Avci O, Abdeljaber O, Kiranyaz S, Hussein M, Gabbouj M, Inman DJ. A review of vibration-based damage detection in civil structures: From traditional methods to Machine Learning and Deep Learning applications. Mech Syst Signal Process 2021;147:107077. https://doi.org/10.1016/j.ymssp.2020.107077.

[3] Farrar CR, Worden K. An Introduction to Structural Health Monitoring, 2010, p. 1–17. https://doi.org/10.1007/978-3-7091-0399-9_1.

[4] Sohn H, Farrar CR, Hemez F, Czarnecki J. A Review of structural health. LibraryLanlGov 2001:1–7.

[5] Soleymani A, Jahangir H, Nehdi ML. Damage detection and monitoring in heritage masonry structures: Systematic review. Constr Build Mater 2023;397:132402. https://doi.org/10.1016/j.conbuildmat.2023.132402.

[6] Kaveh A, Hoseini Vaez SR, Hosseini P. Enhanced vibrating particles system algorithm for damage identification of truss structures. Sci Iran 2019;26:246–56.

[7] Xia Y, Hao H. Statistical damage identification of structures with frequency changes. J Sound Vib 2003;263:853–70. https://doi.org/10.1016/S0022-460X(02)01077-5.

[8] Daneshvar MH, Saffarian M, Jahangir H, Sarmadi H. Damage identification of structural systems by modal strain energy and an optimization-based iterative regularization method. Eng Comput 2023;39:2067–87. https://doi.org/10.1007/s00366-021-01567-5.

[9] Soleymani A, Jahangir H, Rashidi M, Mojtahedi FF, Bahrami M, Javanmardi A. Damage Identification in Reinforced Concrete Beams Using Wavelet Transform of Modal Excitation Responses. Buildings 2023;13:1955. https://doi.org/10.3390/buildings13081955.

[10] Hamdy O, Nawar MT. Damage Detection in Members and Connections of Plane Frame with Flexible Connections Using Residual Force Method and Whale Optimization Algorithm. Iran J Sci Technol Trans Civ Eng 2024;48:1917–31. https://doi.org/10.1007/s40996-023-01316-2.

[11] Jahangir H, Hasani H, dos Santos JVA, Lopes HM. A Comprehensive Study on the Selection of Mother Wavelets and Mode Shapes for Multiple Damage Identification. Iran J Sci Technol Trans Civ Eng 2024;48:1313–27. https://doi.org/10.1007/s40996-024-01394-w.

[12] Ghodrati Amiri G, Seyed Razzaghi SA, Bagheri A. Damage detection in plates based on pattern search and Genetic algorithms. Smart Struct Syst 2011;7:117–32. https://doi.org/10.12989/sss.2011.7.2.117.

[13] Friswell MI, Mottershead JE. Finite Element Model Updating in Structural Dynamics. vol. 38. Dordrecht: Springer Netherlands; 1995. https://doi.org/10.1007/978-94-015-8508-8.

[14] Khanahmadi M, Khalighi M. Interfacial Debonding Detection in Concrete-Filled Steel Tubular (CFST) Columns with Modal Curvature-Based Irregularity Detection Indices. Int J Struct Stab Dyn 2024;24. https://doi.org/10.1142/S0219455424501487.

[15] Kaveh A, Vaez SRH, Hosseini P, Fallah N. Detection of damage in truss structures using Simplified Dolphin Echolocation algorithm based on modal data. Smart Struct Syst 2016;18:983–1004.

[16] Khanahmadi M, Mirzaei B, Dezhkam B, Rezaifar O, Gholhaki M, Amiri GG. Vibration-based health monitoring and damage detection in beam-like structures with innovative approaches based on signal processing: A numerical and experimental study. Structures, vol. 68, Elsevier; 2024, p. 107211. https://doi.org/10.1016/j.istruc.2024.107211.

[17] Khanahmadi M, Mirzaei B, Amiri GG, Gholhaki M, Rezaifar O. Vibration-based damage localization in 3D sandwich panels using an irregularity detection index (IDI) based on signal processing. Meas J Int Meas Confed 2024;224:113902. https://doi.org/10.1016/j.measurement.2023.113902.

[18] Fakharian P, Naderpour H. Damage Severity Quantification Using Wavelet Packet Transform and Peak Picking Method. Pract Period Struct Des Constr 2022;27:4021063. https://doi.org/10.1061/(asce)sc.1943-5576.0000639.

[19] Naderpour H, Fakharian P. A synthesis of peak picking method and wavelet packet transform for structural modal identification. KSCE J Civ Eng 2016;20:2859–67. https://doi.org/10.1007/s12205-016-0523-4.

[20] Azimi M, Eslamlou AD, Pekcan G. Data-driven structural health monitoring and damage detection through deep learning: State-ofthe- art review. Sensors (Switzerland) 2020;20. https://doi.org/10.3390/s20102778.

[21] Kaveh A, Shabani Rad A. Metaheuristic-based optimal design of truss structures using algebraic force method. Structures, vol. 50, Elsevier; 2023, p. 1951–64. https://doi.org/10.1016/j.istruc.2023.02.123.

[22] Ruiz DV, Bragança CSC de, Poncetti BL, Bittencourt TN, Futai MM. Vibration-based structural damage detection strategy using FRFs and machine learning classifiers. Structures 2024;59:105753. https://doi.org/10.1016/j.istruc.2023.105753.

[23] Kourehli SS. Structural Damage Detection under Short Time Load Using Cascade-Forward Network. J Rehabil Civ Eng 2024;12:32–42. https://doi.org/10.22075/jrce.2023.31320.1885.

[24] Yang M, Zhong H. Damage detection for plate-like structures using generalized curvature mode shape method. Earth Sp 2018 Eng Extrem Environ - Proc 16th Bienn Int Conf Eng Sci Constr Oper Challenging Environ 2018;6:1078–87. https://doi.org/10.1061/9780784481899.101.

[25] Hoseini Vaez SR, Fallah N. Damage Detection of Thin Plates Using GA-PSO Algorithm Based on Modal Data. Arab J Sci Eng 2017;42:1251–63. https://doi.org/10.1007/s13369-016-2398-6.

[26] Mohamadinasab M, Amiri GG, Dehcheshmeh MM. Structural Damage Detection of Symmetric and Asymmetric Strutures Using Different Objective Functions and Multiverse Optimizer. Iran Univ Sci Technol 2023;13:391–411. https://doi.org/10.22068/ijoce.2023.13.4.563.

[27] Fan W, Qiao P. A 2-D continuous wavelet transform of mode shape data for damage detection of plate structures. Int J Solids Struct 2009;46:4379–95. https://doi.org/10.1016/j.ijsolstr.2009.08.022.

[28] Xiang J, Liang M. A two-step approach to multi-damage detection for plate structures. Eng Fract Mech 2012;91:73–86. https://doi.org/10.1016/j.engfracmech.2012.04.028.

[29] Seyedpoor SM, Yahyapour R, Mofdi AA, Fallahian S. Structural Damage Identification through an Optimal Sensor Placement Approach and the Modal Strain Energy Based Index. J Rehabil Civ Eng 2024;12. https://doi.org/10.22075/jrce.2023.29823.1805.

[30] Mohamadi Dehcheshmeh M, Amiri GG, Zare Hosseinzadeh A, Torbatinejad V. Structural damage detection based on modal data using moth-flame optimization algorithm. Proc Inst Civ Eng - Struct Build 2019:1–43. https://doi.org/10.1680/jstbu.18.00121.

[31] Mueller DW. An introduction to the finite element method using MATLAB. Int J Mech Eng Educ 2005;33:260–77. https://doi.org/10.7227/IJMEE.33.3.8.

[32] Reddy JN. An Introduction to the Finite Element Method 1993.

[33] Timoshenko S. Goodier. JN, Theory of Elasticity. New York McGraw—Hil1 1970;970:279–91.

[34] Zienkiewicz OC, Taylor RL. The finite element method for solid and structural mechanics. Elsevier; 2005.

[35] Khanahmadi M. An effective vibration-based feature extraction method for single and multiple damage localization in thin-walled plates using one-dimensional wavelet transform: A numerical and experimental study. Thin-Walled Struct 2024;204:112288. https://doi.org/10.1016/j.tws.2024.112288.

[36] Bucolo M, Caponetto R, Fortuna L, Frasca M, Rizzo A. Does chaos work better than noise? IEEE Circuits Syst Mag 2002;2:4–19.

[37] Ott E, Wiesenfeld K. Chaos in Dynamical Systems . vol. 47. Cambridge university press; 1994. https://doi.org/10.1063/1.2808369.

[38] Talatahari S, Azizi M. Chaos Game Optimization: a novel metaheuristic algorithm. Artif Intell Rev 2021;54:917–1004. https://doi.org/10.1007/s10462-020-09867-w.

[39] Kaur G, Arora S. Chaotic whale optimization algorithm. J Comput Des Eng 2018;5:275–84. https://doi.org/10.1016/j.jcde.2017.12.006.

[40] Rao R V., Savsani VJ, Vakharia DP. Teaching-learning-based optimization: A novel method for constrained mechanical design optimization problems. CAD Comput Aided Des 2011;43:303–15. https://doi.org/10.1016/j.cad.2010.12.015.